Chapter 7
Tension Control in a Steel Slitting Line

Gregor Dolanc

7.1 Introduction

Steel slitting lines are used to slice wide steel strips which come out of a cold rolling mill into a number of narrower strips of the width specified by the customer. The tension of the steel strip in front of the slitter is one of the key technological parameters that affect the quality of the slitting process. This chapter describes a steel strip tension control system which was developed in the framework of reengineering an existing steel slitting line in a cold rolling mill.

The motivation for the reengineering project was the following. In the steel plant discussed below there were two steel slitting lines, one for processing the thinner material and the other for the thicker material. Over time, market demands have changed in favour of the thinner material, which is used for more advanced products and is therefore priced higher than the thicker material. In order to meet increased market demands, it was necessary to significantly increase the production capacity of the thinner material. One option was to install an additional new line for processing the thinner material, but this idea was abandoned due to the consequent high financial and logistical burden on the company. On the other hand, the line producing the thicker material was operating at around 50 % capacity, and therefore a much better idea was to utilise the remaining capacity for the production of the thinner material. For that purpose, the entire line had to be thoroughly reengineered.

An additional motivation for reengineering the line was to increase reliability and reduce maintenance costs. The existing control system was already more than 30 years old and was based on obsolete analogue electronic circuits. This resulted in reduced reliability and increased the number of maintenance interventions. The only remedy for this situation was to replace the existing system with a new computer-based control system.

Reengineering and functional modifications of the existing control system represented a great challenge because we wanted to expand the slitting line functionality

G. Dolanc (✉)
Department of Systems and Control, Jožef Stefan Institute, Ljubljana, Slovenia

S. Strmčnik, Đ. Juričić (eds.), *Case Studies in Control*, Advances in Industrial Control,
DOI 10.1007/978-1-4471-5176-0_7,

by means of advanced control solutions rather than expensive mechanical modifications. This chapter is focused on the theoretical background of the steel strip tension control part of the control system, and also on the most relevant practical aspects of implementation, which significantly contributed to the success of the entire project.

The remaining part of the chapter is organised as follows. In the next section, the steel slitting line and main functional requirements of the control system are described. Then we focus on the problem of steel strip tension control arising in most steel slitting lines and analyse the possibilities for solving this problem. We continue with the central goal of this chapter, i.e., the design and implementation of the steel strip tension control system. Finally, we discuss some practical difficulties encountered when applying the theory.

7.2 Description of the Steel Slitting Line and Main Functional Requirements of the Control System

The cold rolling mill under consideration consists of two different slitting lines, one for thinner material and the other for the thicker material, which are shown schematically in Figs. 7.1 and 7.2.

In both lines a steel strip is continuously uncoiled from the uncoiler and led to the rotating slitter. In the slitter it is longitudinally cut into several narrower strips, which are then wound up into coils by the recoiler. The tension of the steel strip between the uncoiler and slitter must be carefully controlled, since this affects the quality of the slitting process.

Processing the thinner material requires very accurate tension control. In the thinner material line the tension is controlled mechanically, i.e., by a combination of a mechanical brake and an entry disburdening loop. Thanks to the loop, the slitter is exposed only to the force of the mechanical brake and is not exposed to the force of the uncoiler.

The processing of the thicker material tolerates less precise tension control in front of the slitter. Therefore, the configuration of the line for the thicker material is simpler. The entry disburdening loop is left out, so that only the exit disburdening loop is present.

The exit disburdening loop and the mechanical brake are used in both lines to control the tension of winding up the sliced steel strips. In addition, the exit loop also compensates for any possible length difference between particular strips which may accumulate during slitting.

DC motors are usually used in drives since their speed and torque are very easily controlled by armature voltage and current. In the line for producing the thicker material 150 kW DC motors are used in the uncoiler and recoiler drives and a 20 kW DC motor is used in the slitter drive. Figure 7.3 shows the mechanical setup of the uncoiler of the slitting line for the thicker material, consisting of the DC motor, gearbox, coil hub and auxiliary equipment.

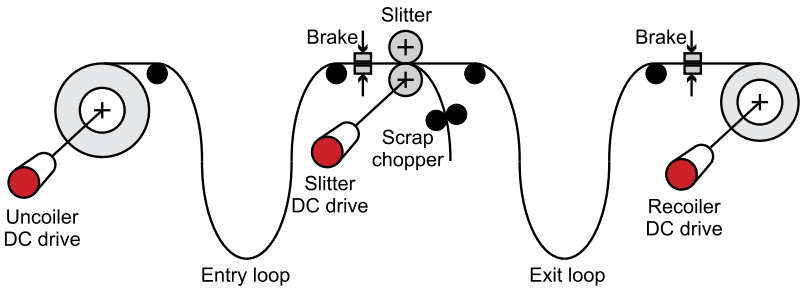

Fig. 7.1 Slitting line for the thinner material

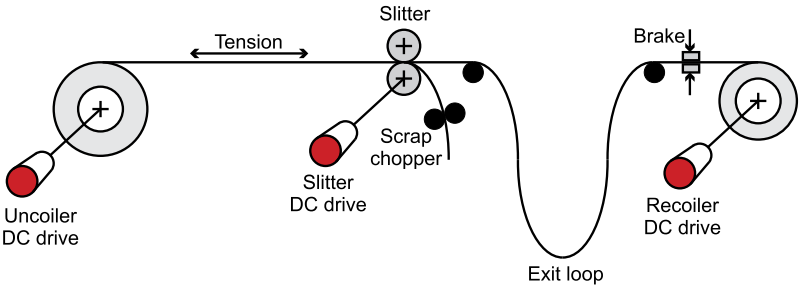

Fig. 7.2 Slitting line for the thicker material

7.2.1 Possible Solutions

The main goal of the project was to increase production of the thinner material. To achieve this, there were several options, as shown in Fig. 7.4.

The first option was to build up an additional new line for the thinner material (option a), but this turned out to be too expensive and logistically demanding.

The alternative and finally accepted approach was to upgrade the existing line originally used for processing the thicker material (option b). The line had to be technologically upgraded to enable the line to also process the thinner material, in particular the tension control between the uncoiler and slitter had to be made more accurate. This could be done in two ways.

The most direct and risk-free solution would be to implement the missing entry disburdening loop (option c). To do this, a mechanical setup very similar to the setup of the existing exit loop (shown in Fig. 7.5 and Fig. 7.6, C) would have to be implemented between the uncoiler and the slitter. However, among other matters, this would require approximately 5 meters of additional space between the uncoiler (Fig. 7.6, A) and the slitter (Fig. 7.6, B). To provide the space, the position of the uncoiler with all the associated equipment and installations would have to be rearranged. This would lead to very expensive and complicated modifications.

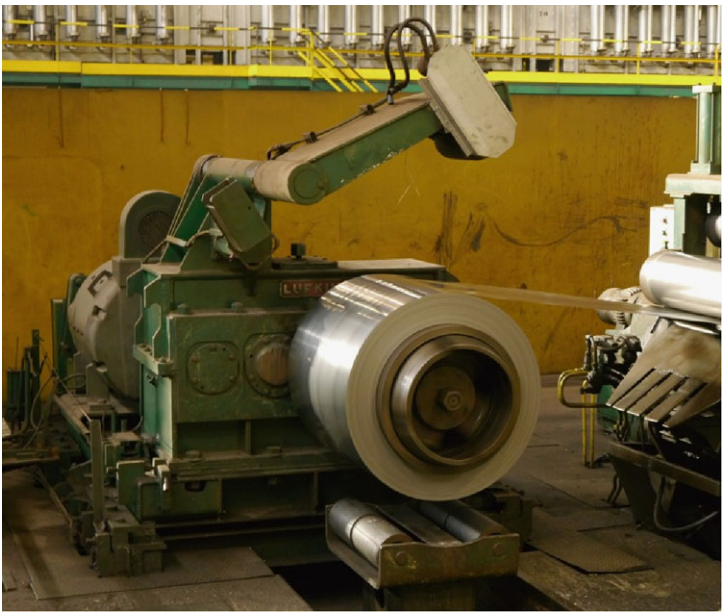

Fig. 7.3 Mechanical setup of the uncoiler (150 kW DC drive)

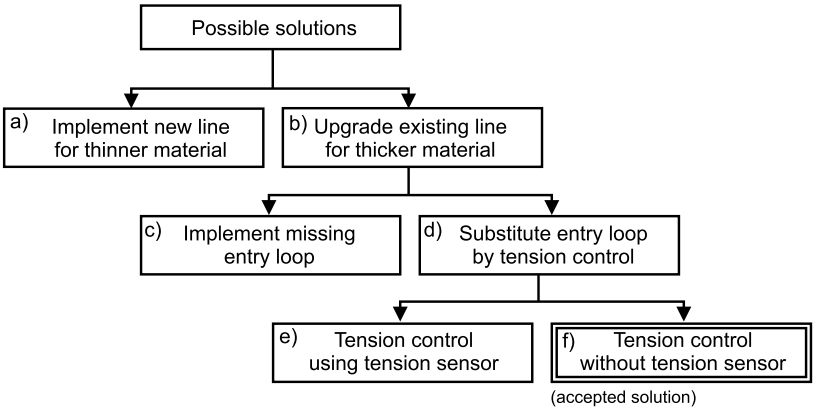

Fig. 7.4 Possible solutions for increasing the production of the thinner material

There was therefore a desire to avoid modifications to the mechanical setup and to substitute for the missing disburdening loop by controlling the tension via electric variables of the drives (option d).

This kind of tension control is usually based on measuring the tension with a sensor (option e) and controlling the drive torque. However, the installation of a tension sensor into the existing line would still require significant mechanical modifications, so there was a desire to omit the tension sensor too. The remaining option was to

Fig. 7.5 Mechanical setup of the exit loop between the slitter and the recoiler

control the tension without a tension sensor by a combined feedback and feedforward control scheme (option f), which will be described in more detail below.

7.2.2 The Previous Control System

The previous version of the control system was implemented using analog electronic circuits and enabled the following operation modes: slitting mode, rewinding mode without slitting, and several modes of jog operation used to feed the steel strip into the line or to resolve irregular events. The existing slitting mode was implemented by controlling the drives in the following way:

- The slitter DC drive operated in linear speed control mode, which means that the slitter determined the speed of the steel strip.
- The uncoiler DC drive operated in tension control mode, which means that the tension of the steel strip between the uncoiler and the slitter was held at an approximately constant value. Tension was controlled via the uncoiler motor armature current, however, the control was pretty rough, especially during acceleration/deceleration. The control did not take into account the variable coil radius.

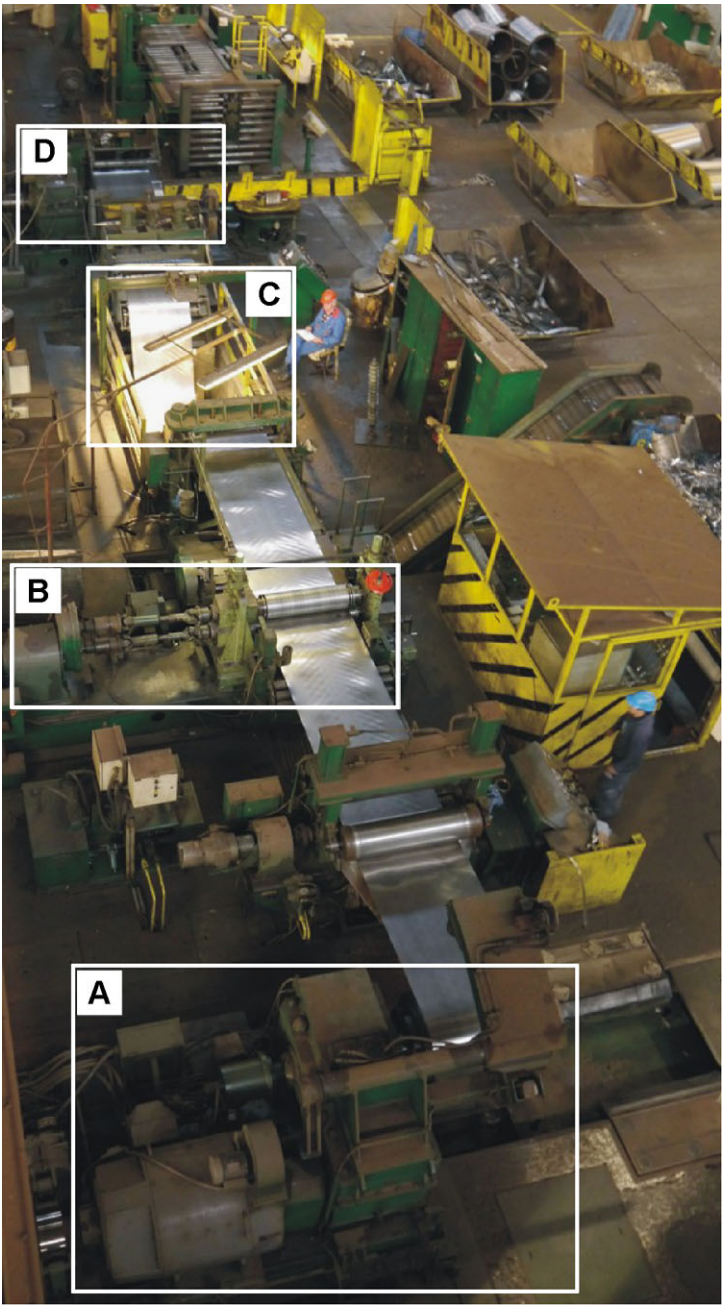

Fig. 7.6 The steel strip slitting line for the thicker material which was subject to modernization (**A**—uncoiler, **B**—slitter, **C**—exit loop, **D**—recoiler)

Consequently, tension was not constant during a speed change. This was not so problematic during processing the thicker material, but would become an important issue during processing of the sensitive thinner material.
- The recoiler DC drive operated in linear speed control mode. The operator had to maintain the level of the exit loop by manually correcting the uncoiler speed set-point via the potentiometer.

7.2.3 Requirements for the New Control System

The goals in upgrading the control system were the following:

- To achieve more accurate control of the tension between the uncoiler and the slitter. In particular, it was very important that the tension remain under control also during acceleration/deceleration. This was essential for processing the thinner material, which is much more sensitive to mechanical stress than the thicker material.
- To achieve automatic control of the exit loop level.
- To replace the existing analogue control circuits with a more reliable and flexible programmable logic controller.

The main idea with regard to upgrading the control system is the following. The required speed of the steel strip remains the main reference signal and is adjusted by the operator. It represents a set-point for the speed controller of the slitter. The slitter remains the master drive and therefore the other drives have to be coordinated with the master one.

The coordination of the slitter and the uncoiler is performed by maintaining a constant tension of the steel strip between the uncoiler and the slitter. Generally, when controlling the tension of the strip between the two drives, both tension and speed must be controlled. Therefore, one of the drives operates in a linear speed control mode dictating the speed, while the other drive operates in a tension control mode. In the slitting line at issue, the slitter operates in linear speed control mode and the uncoiler operates in tension control mode. The direction of the tension of the uncoiler is opposite to the direction of the speed of the steel strip. Therefore, the direction of the uncoiler motor torque is opposite to the direction of the angular speed, which means that the motor operates either in generator mode or active brake mode, depending on the level of the required tension.

The coordination between the slitter and the recoiler is performed by automatically controlling the constant level of the exit disburdening loop, however, this is not a matter addressed in this chapter.

In order to perform the required operation, a generalised control diagram for the DC drive was designed as indicated in Fig. 7.7.

The control diagram in Fig. 7.7 should be implemented for all three drives. The diagram performs basic control of the DC drives and coordination between the drives. Basic control is needed in all drives and includes control of the armature (rotor) current and field (stator) current. The currents are controlled by PI controllers

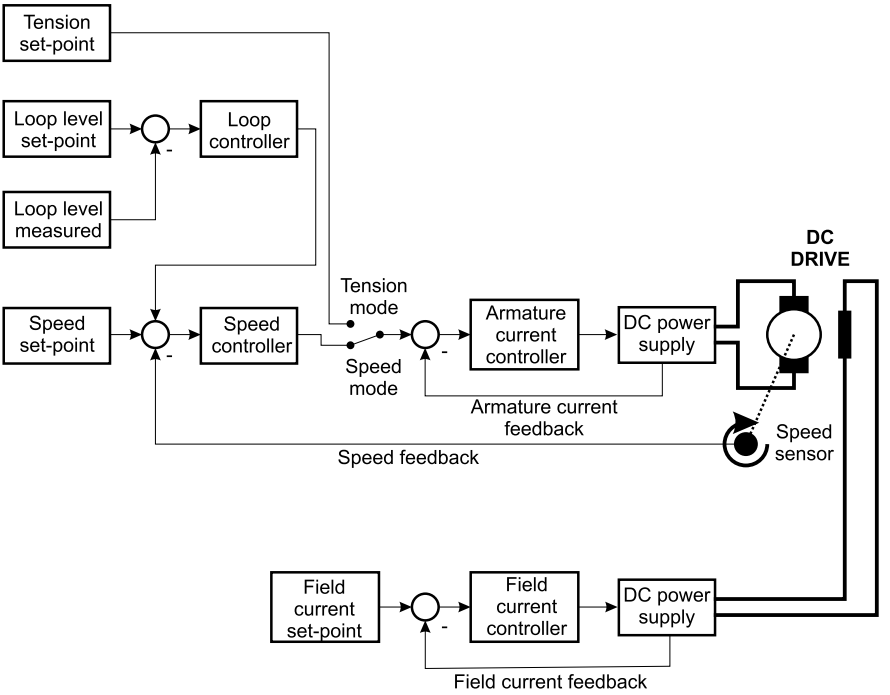

Fig. 7.7 Simplified control diagram of one DC drive

which adjust the voltages of the DC power supplies of the armature and field. The control diagram in Fig. 7.7 provides three possibilities for coordination with other drives: linear speed control, tension control, or loop level control between the two drives. In the remainder of this chapter we will focus on tension control of the steel strip between the uncoiler and the slitter.

7.3 The Steel Strip Tension Control Problem

Maintaining the proper tension is crucial for the quality of the slitting process. In the absence of the disburdening loop, maintaining the proper tension is even more important than in the presence of the disburdening loop. If the tension is too high, the steel strip begins to slip in the slitter, resulting in an uneven cut and damaged slitter knives. On the other hand, if the tension is too low or zero, the steel strip becomes loose, which leads to poor lateral guidance of the strip and eventually it will run out of the track. Additionally, an uncontrolled strip loop may begin to appear between the uncoiler and the slitter and this may cause bumps while re-establishing the tension, which almost certainly leads to damaged slitter knives. Therefore, the tension must always be close to some low set-point value and this is particularly important when processing the thinner material, which is more sensitive to mechanical

stress. The tension must be held constant not only when the speed is constant, but also during acceleration and deceleration and jog operation.

7.3.1 Main Requirements and Ideas for Possible Solutions

The idea was to control the tension by controlling the slitter drive linear speed and uncoiler drive torque. The latter is proportional to the motor armature current. However, the relationship between the motor torque and the tension is nonlinear for various reasons. Firstly, at constant speed the relationship between tension and torque varies with the uncoiler coil radius, which decreases due to the uncoiling of the steel strip. Secondly, during speed change, a part of the motor torque is utilised to accelerate or decelerate the rotating masses (coil, motor, gear). In order to control the tension, it is obvious that the torque for the acceleration/deceleration of the rotating masses must be taken into account. This can be accomplished by a feedforward compensator, which should be a part of the control block diagram. Note that for precise tension control the compensator parameters must be carefully tuned. A prerequisite to implementing this kind of tension control is "four quadrant operation" of the armature DC power supply of the drive controlling the tension. This means that the drive can rotate in both directions in motor mode, generator mode and active brake mode.

7.3.2 Relation to the Existing Solutions

Tension control is one of the most common control problems in steel slitting lines as well as in web processing machines. Tension is usually controlled by simultaneous control of several electric drives. Due to the significant practical relevance, problems of this kind have been widely discussed in the literature. The fundamentals of dynamic modelling and control in web processing machines are given in, e.g., [11], where basic control diagrams for speed and tension control are presented. In general, web tension can be measured by sensors, such as load cells or dancer rolls [6], however, their installation requires extensive mechanical modifications. An alternative is to estimate tension by observers. This can be done in several ways, depending on the type of machine and the properties of the web. In [9] the authors developed three types of observers for tension estimation in web winding machines. The first type of observer is a nonlinear observer that estimates the tension between two drives by using the difference between their linear speeds. The speed difference is a result of web prolongation due to elasticity, considering also the effect of inertia. This approach is expected to work well provided the elasticity of the web is significant (e.g., in the case of rubber, plastic materials, paper). In our case, the prolongation of the steel strip is relatively low due to the low elasticity of steel and the short length of the strip segment between the uncoiler and the slitter. This would lead to a low

speed difference between the drives which cannot be measured accurately enough. In addition, due to the slitting process, the linear speed of the slitter is slightly higher than the actual speed of the steel strip. For these reasons, the proposed nonlinear observer is not expected to work in our case. The other two approaches stressed in [9] refer to an algebraic observer and a sliding-mode observer, which estimate the tension from the torques generated by the drives. This can work also for lower or zero web elasticity but, unfortunately, cannot be directly used in our case. The reason is that a significant part of the torque generated by the slitter is consumed for cutting and reshaping the material.

In [12] three different tension control methods are tested on a prototype machine, consisting of two drives, one operating in tension mode and the other operating in speed mode. The first method consists of an open loop tension controller with feedforward compensation of the acceleration and deceleration torque, which is related to our solution, but designed for AC drives only. The second method consists of a classical cascade control in which the tension is directly measured by the tension sensor. The tension controller corrects the speed reference of the linear speed controller of the first drive. As explained, the use of a tension sensor was an unfavourable option in our case due to the mechanical complications of the installation. The third method utilises a tension observer which estimates the tension based on the motor torque generated and the measured drive speed and acceleration. This is a classical feedback control scheme with a tension sensor substituted for by the observer and does not incorporate feedforward compensation, which is needed in our case.

Several industrial case studies are reported in the literature, most often in association with hot and cold rolling mills in the steel industry, as well as in association with different kinds of paper production machines. A survey of tension control methods for rolling mills can be found in [4]. However, tension control in rolling mills is not directly comparable to tension control in slitting lines, since rolling mill operation requires more accurate tension control than slitting lines. Due to the high precision demands, the tension in rolling mills is usually measured by tension sensors and controlled by a feedback loop. Similar tension control applications can also be found in paper production machines. During operation, a paper strip runs through the production machines with many coils and drives, and the tension between them has to be controlled. Several reports exist in the literature in which sensorless tension control is applied to paper machines, e.g., [3, 7], but the presented systems are based on AC drives. In our case, the whole system is based on DC drives, which leads to different control structures.

7.3.3 Why a Commercially Available Solution Was Not Applicable

Nowadays, many systems for the coordinated control of electric drives are commercially available. Solutions exist for DC drives and AC drives. In cases where speed control or torque control was required, or coordination between multiple drives had

to be established, DC drives were traditionally dominant, since their speed and torque can be controlled very elegantly via armature voltage and current [1, 10]. On the contrary, AC drives were originally used only in applications where controlled or coordinated operation was not required. Conditions changed dramatically after the introduction of AC frequency converters and servo controllers. At their early stage of development, AC frequency converters were only available for a low power range and were only capable of adjusting the speed of the motor in an open loop via the frequency of the AC voltage. As their development progressed, frequency converters also became available in higher power ranges (>100 kW) and they began to support more advanced control functions, such as closed loop speed control, torque limitation/control, and position control. Due to expanded functionality, relatively low costs, simple mechanical design, and low maintenance costs, AC drives invaded many areas previously dominated by DC motors, e.g., the paper industry, the metal industry, and many other fields. Nowadays, some manufacturers of electric motors and drives also offer accompanying hardware equipment (power converters along with programmable control units) and control software (programming tools and libraries of function blocks) to implement various control functions related to motor drive operation. The technology for DC and AC drives exists on the market, although AC drives predominate for the mentioned reasons of increased functionality and low cost design. In spite of the available technology, we decided to implement a custom-oriented solution for the following reasons:

- In order to gain benefits from the state-of-the-art control hardware and software for electric drives, the DC power supplies in the existing line would have to be replaced, too. The reason is that drive-related control functions are usually integrated within state-of-the-art DC power supplies, which nowadays combine both a rectifier unit and a programmable control unit. In the project considered, the existing DC power supplies remained in service since their replacement would have required relatively high additional costs. Thus, new control functions had to be implemented outside the DC power supplies, using an external programmable logic controller.
- We wanted to provide a completely custom-made solution which would be perfectly adapted to the existing system and to the particular technological demands. This is only possible if all control functions are developed "from scratch".
- By omitting mechanical modifications and by using general purpose control hardware and software, it was possible to provide a low-cost solution and simultaneously to achieve the required increase in the functionality of the slitting line.

7.4 Design of Steel Strip Tension Control

7.4.1 Model of the DC Drive

The typical DC drive consists of a DC motor and a gearbox. High power DC motors are externally excited, which means that the magnetic flux is generated by a DC

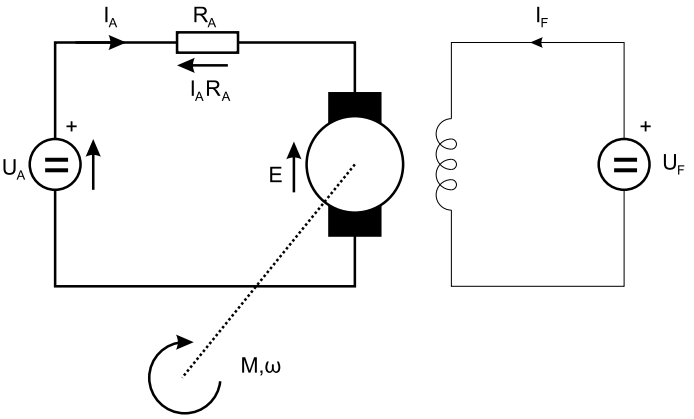

Fig. 7.8 Simplified scheme of the DC motor with external excitation

current through the stator coil. The simplified electric scheme is shown in Fig. 7.8. The principle of operation and associated physical relations can be found in many textbooks, e.g., [5], and here only the main relationships will be outlined.

The DC motor is controlled by two input variables: the armature DC voltage U_A and the stator DC current I_F, which is controlled via field DC voltage U_F. The controlled outputs are the angular velocity ω and torque M generated due to the force between the rotor and the stator.

The armature voltage U_A covers a voltage drop at the armature resistance R_A and the back electromotive force E

$$U_A = I_A R_A + E \tag{7.1}$$

The back electromotive force (also denoted as *EMF*) is caused by armature rotation through the magnetic field and is proportional to the armature angular speed ω and the magnetic flux ϕ (field), generated by the stator

$$E = k_0 \phi \omega \tag{7.2}$$

Here, k_0 is a dimensionless proportional constant. In DC motors with external excitation, the magnetic flux ϕ is generated by a stator coil and is proportional to the current through the stator coil, referred to as field current I_F

$$\phi = I_F k_F \tag{7.3}$$

where factor k_F [Vs/A] depends on the motor construction parameters. The motor torque is proportional to both the armature current I_A and magnetic flux ϕ

$$M = k_0 \phi I_A \tag{7.4}$$

Since the flux is proportional to the field current I_F, the motor torque reads

$$M = k_0 k_F I_A I_F \tag{7.5}$$

The armature current I_A is proportional to the voltage difference $(U_A - E)$ that drives it and inversely proportional to the armature resistance R_A

$$I_A = \frac{U_A - E}{R_A} \tag{7.6}$$

By combining Eqs. (7.2), (7.3), and (7.6), the armature current can be expressed as a function of the armature voltage U_A and the angular speed ω

$$I_A = \frac{U_A - k_0 \phi \omega}{R_A} = \frac{U_A - k_0 k_F I_F \omega}{R_A} \tag{7.7}$$

Provided the armature current I_A is known, the angular speed ω reads

$$\omega = \frac{U_A - I_A R_A}{k_0 k_F I_F} \tag{7.8}$$

Using Eqs. (7.5) and (7.7), the motor torque M can be expressed as a function of the armature voltage U_A, field current I_F, and angular velocity ω

$$M = k_0 k_F I_F I_A = k_0 k_F I_F \cdot \frac{U_A - k_0 k_F I_F \omega}{R_A} = \frac{k_0 k_F I_F U_A - (k_0 k_F I_F)^2 \omega}{R_A} \tag{7.9}$$

One can see that the field current I_F performs similarly to a continuously adjustable gear: increasing the field current results in reduced motor speed ω and increased torque M and vice versa.

All relations presented up to this point are static. They are valid only in the case of operation at constant speed. Let us now analyse the dynamic relation between the armature voltage U_A and the motor angular speed ω. To do this, let us first consider the generated motor torque. It is utilised to accelerate the rotating masses with moment of inertia J, to compensate for the friction torque $(k_{FR}\omega)$ and external load torque M_F

$$M = J\dot{\omega} + k_{FR}\omega + M_F \tag{7.10}$$

At the same time, the generated motor torque depends on the armature voltage and motor angular speed, as follows from Eq. (7.9). After combining the relations (7.9) and (7.10), we obtain a first order linear differential equation for angular speed ω

$$J\dot{\omega} + \left(\frac{(k_0 k_F I_F)^2}{R_A} + k_{FR} \right) \omega = \frac{k_0 k_F I_F U_A}{R_A} - M_F \tag{7.11}$$

Now let us analyse the moment of inertia J of the rotating masses, which are accelerated by the motor. Recall that all DC drives of the slitting line are composed of a DC motor and a gearbox (Fig. 7.9).

Let the gear ratio be denoted as G. In the case of the considered drives, G is greater than 1. The input shaft of the gear (at the motor side) rotates with speed ω

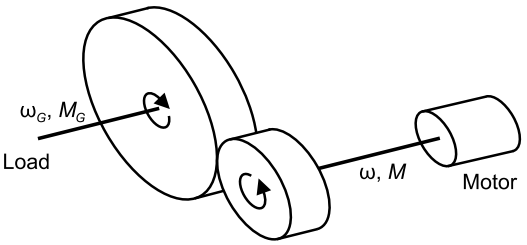

Fig. 7.9 DC drive with a motor and a gearbox

while the output shaft rotates with the reduced speed ω_G

$$\omega_G = \frac{\omega}{G} \tag{7.12}$$

The motor provides the torque M, while the output shaft of the gearbox delivers increased torque M_G

$$M_G = MG \tag{7.13}$$

To determine the effective moment of inertia J, it is necessary to evaluate the moment of inertia of the complete system (motor + gearbox + other rotating masses). Let the components of the moment of inertia be divided into two parts:

- J_M—the moment of inertia of all parts rotating with speed ω (the rotor, the primary part of the gear)
- J_L—the moment of inertia of all parts rotating with speed ω_G (the secondary part of the gear, the steel strip coil).

The moment of inertia J_L is reflected to the motor side via the gear by the factor $(1/G^2)$. Therefore, the total moment of inertia on the motor side is

$$J = J_M + \frac{J_L}{G^2} \tag{7.14}$$

In the case of the uncoiler DC drive, the moment of inertia J_L can be subsequently divided into two components

$$J_L = J_H + J_C \tag{7.15}$$

where

- J_H is the constant moment of inertia of the uncoiler hub element, axis and load side of the gear;
- J_C is a variable moment of inertia of the still strip coil with variable radius and mass (due to steel strip uncoiling).

Now let us determine the moment of inertia of the steel strip coil, which is shown in Fig. 7.10 and geometrically represents a “thick wall tube”.

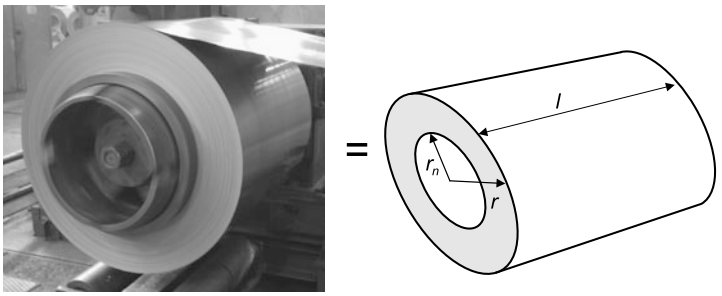

Fig. 7.10 Steel strip coil

The moment of inertia of such a geometric body is expressed as

$$J_C = \frac{m}{2}\left(r^2 + r_n^2\right) \tag{7.16}$$

Here, m represents the mass, r_n is the internal radius (constant), and r is the outside radius (variable). Furthermore, the mass can be expressed as a product of the density ρ and the volume V, the latter is a function of the variable outside radius r, the internal radius r_n, and the width l

$$V = \pi\left(r^2 - r_n^2\right)l \tag{7.17}$$

Thus the mass is

$$m = \rho V = \rho\pi\left(r^2 - r_n^2\right)l \tag{7.18}$$

If Eq. (7.18) is put into Eq. (7.16), we obtain the coil moment of inertia expressed as a function of the geometric dimensions

$$J_C = \frac{\pi l\rho}{2}\left(r^4 - r_n^4\right) \tag{7.19}$$

Considering relations (7.15) and (7.19), we can rewrite expression (7.14) for the total moment of inertia, which is a function of the variable radius r of the steel strip coil

$$J = \frac{\pi l\rho}{2G^2}\left(r^4 - r_n^4\right) + \frac{J_H}{G^2} + J_M \tag{7.20}$$

7.4.2 Linear Speed Control

A very common mode of operation is the control of linear speed (in our case, linear speed is the speed of the steel strip). The linear speed v depends on the motor angular

speed ω, the gear ratio G, and the outside radius r of the coil or roll which drives the steel strip

$$v = \omega_G r = \frac{\omega r}{G} \tag{7.21}$$

If we consider the relation (7.8) in (7.21) in a steady state, we obtain

$$v = \frac{(U_A - I_A R_A) r}{G k_0 k_F I_F} \tag{7.22}$$

Since the radius r of the uncoiler and recoiler coil varies with time, the gain between the armature voltage U_A and the linear speed v is not constant but increases with the radius r. Variable gain in general requires variable parameters of the controller (e.g., PI) for linear speed, which would complicate the control structure. However, we can make the gain constant by eliminating the coil radius from Eq. (7.22). This can be done by adjusting the field current I_F in the following way:

$$I_F = k_R r \tag{7.23}$$

where k_R is the proportional factor [A/m] of the control system. To implement this relation, the coil radius has to be measured online by a sensor. By inserting Eq. (7.23) into Eq. (7.22), the coil radius r is eliminated. As a result, the linear speed only depends on the armature voltage and current, as follows from Eq. (7.24):

$$v = \frac{(U_A - I_A R_A)}{G k_0 k_F k_R} \tag{7.24}$$

7.4.3 Tension Control

Let us analyse the relation between the motor armature current I_A and tension force F of the steel strip. We start with the generated motor torque M, which can be decomposed into two components, M_F and M_A,

$$M = M_F + M_A \tag{7.25}$$

The first component M_F represents the torque which generates the tension force F of the steel strip. The tension force causes the torque $F \cdot r$ at the uncoiler coil with radius r and this torque divided by the gear ratio must equal the motor torque M_F

$$M_F = \frac{F r}{G} \tag{7.26}$$

The second component M_A represents the torque needed for the acceleration/deceleration of the rotating masses

$$M_A = J \dot{\omega} \tag{7.27}$$

Here J stands for the moment of inertia, given by Eq. (7.20), and $\dot{\omega}$ is the motor angular acceleration. Taking into account the coil radius r and gear ratio G, a link between the motor angular acceleration $\dot{\omega}$ and the linear acceleration $\dot{v}$ of the steel strip can be expressed as

$$\dot{\omega} = \frac{\dot{v}}{r} G \tag{7.28}$$

If this relation is inserted into Eq. (7.27), we obtain the relation between the motor torque and the linear acceleration

$$M_A = J \frac{\dot{v}}{r} G \tag{7.29}$$

The motor has to overcome both components, M_F and M_A, by generating the torque M according to Eq. (7.5). As in linear speed control mode, we apply the same relation (7.23) between the coil radius r and the field current I_F. In this way we compensate for the effect of the variable coil radius in the relation between the armature current and the tension of the steel. With this in mind, the torque generated by the motor reads

$$M = I_A k_0 k_F k_R r \tag{7.30}$$

By considering relations (7.26), (7.29), and (7.30) in (7.25), we get

$$I_A k_0 k_F k_R r = \frac{Fr}{G} + J \frac{\dot{v}}{r} G \tag{7.31}$$

From relation (7.31), we can express the armature current I_A, which generates the tension F of the steel strip and accelerates the rotating masses by the acceleration $\dot{v}$

$$I_A = \frac{1}{k_0 k_F k_R} \left(\frac{F}{G} + \frac{JG\dot{v}}{r^2} \right) \tag{7.32}$$

As with the torque, also the relation for the armature current (7.32) can be decomposed into two components, I_{AF} and I_{AA}. Let us call the first component I_{AF} the "tension current", generating the demanded tension force F

$$I_{AF} = F \frac{1}{k_0 k_F k_R G} = F k_A \tag{7.33}$$

We see that the gain k_A between the tension F and the armature current I_{AF} is constant despite the variable coil radius r. This is a consequence of relation (7.23) acting as a linearisation.

The second component I_{AA} is referred to as the "acceleration current" generating the torque M_A for the acceleration of the rotating masses of the uncoiler with overall moment of inertia J

$$I_{AA} = \dot{v} \frac{JG}{k_0 k_F k_R r^2} = \dot{v} f(r) \tag{7.34}$$

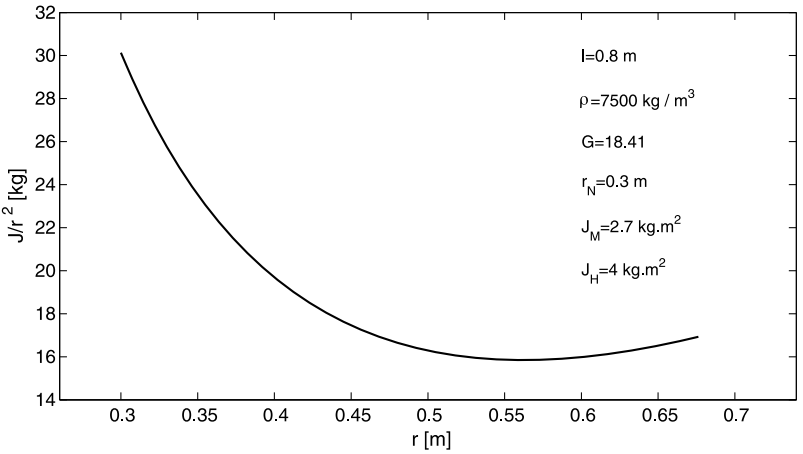

Fig. 7.11 The term J/r^2 as a function of the coil radius r

where $f(r)$ is

$$f(r) = \frac{G}{k_0 k_F k_R} \cdot \frac{J}{r^2} \tag{7.35}$$

Equation (7.34) is used to determine the armature current needed for the required acceleration. So the linear acceleration $\dot{v}$ in Eq. (7.34) actually represents the required acceleration $\dot{v}_{DEM}$. It must match as closely as possible the actual acceleration of the drive controlling the speed, i.e., the slitter drive, which operates in linear speed control mode. In Eq. (7.35) the term J/r^2 appears, which can be expressed by dividing Eq. (7.20) by r^2

$$\frac{J}{r^2} = \frac{\pi l \rho}{2G^2}\left(r^2 - \frac{r_n^4}{r^2}\right) + \frac{J_H}{G^2 r^2} + \frac{J_M}{r^2} \tag{7.36}$$

An example of function (7.36) is represented in Fig. 7.11. Note that the position of the minimum of function (7.36) depends on its parameters and it may appear outside the operating range of the radius.

Relations (7.33), (7.34), (7.35), and (7.36) represent the background for the DC drive control block diagram, which will be discussed in the next section. The relation (7.33) between the armature current and tension in general requires the DC drive parameters to be known with sufficient accuracy. The mitigating fact in our case is that the tension set-point is not explicitly prescribed in terms of a strict numerical value. Instead, based on experience and visual feedback (observing the sag of the steel strip, see Fig. 7.12), the operator adjusts the tension set-point to optimise the slitting process and guidance of the steel strip. Sagging of a few centimetres indicates the correct tension. Once the tension set-point is properly adjusted, the actual tension is automatically controlled by the control system and operator intervention is no longer required.

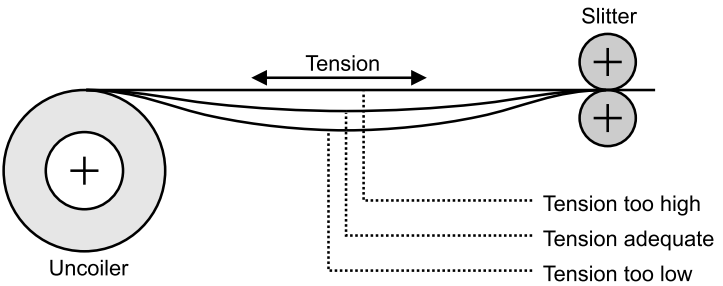

Fig. 7.12 Adjusting the tension set-point

7.4.4 Block Diagram of the DC Drive Control

Figure 7.13 represents the control diagram in a simplified form. It is composed of feedforward and feedback blocks. The tension set-point F is adjusted by the operator via the potentiometer. It is set to some low negative value so that the actual tension is opposite to the direction of the linear speed. The input $\dot{v}_{DEM}$ represents the required acceleration. As we have already explained, it should be as close as possible to the actual acceleration of the slitter drive operating in linear speed control mode. In Sect. 7.4.5 we will show how the actual acceleration of the slitter is estimated. Based on the required tension F, required acceleration $\dot{v}_{DEM}$, and measured coil radius r, the tension current I_{AF} is determined by the feedforward relation (7.33) and the acceleration current I_{AA} by the feedforward relations (7.34), (7.35), and (7.36). The sum of the components I_{AF} and I_{AA} represents the armature current set-point I_{AT} for tension control mode. Based on this set-point, the armature current is then controlled by a feedback (PI) controller, which adjusts the armature voltage command signal U_{A_CMD}. The field current set-point I_{F_SET} is determined by feedforward relation (7.23) and fed into the field current PI controller, which controls the field current by adjusting the field voltage command signal U_{F_CMD}. Note that the field current must never decrease below a certain minimum value, otherwise the motor speed may increase too much and go out of control. Therefore, a safety function (limitation) is implemented, which sets the lower and upper limits of the field current in case of coil radius sensor failure.

The diagram in Fig. 7.13 supports three modes of operation. We will review each of them in more detail.

Tension Mode The selection switch in front of the speed controller is set to the position "armature voltage control" and the selection switch in front of the armature current controller is set to the position "tension control". The armature current set-point I_{AT} is fed via the selection switch into the armature current controller, which controls the actual armature current by adjusting the armature voltage command signal U_{A_CMD}. At the same time, the speed controller is exposed to the safety set-point v_T (low negative value, e.g., -30 % of the maximum armature voltage), which is activated by setting the binary signal *TSPD* to 1 as long as the tension mode is

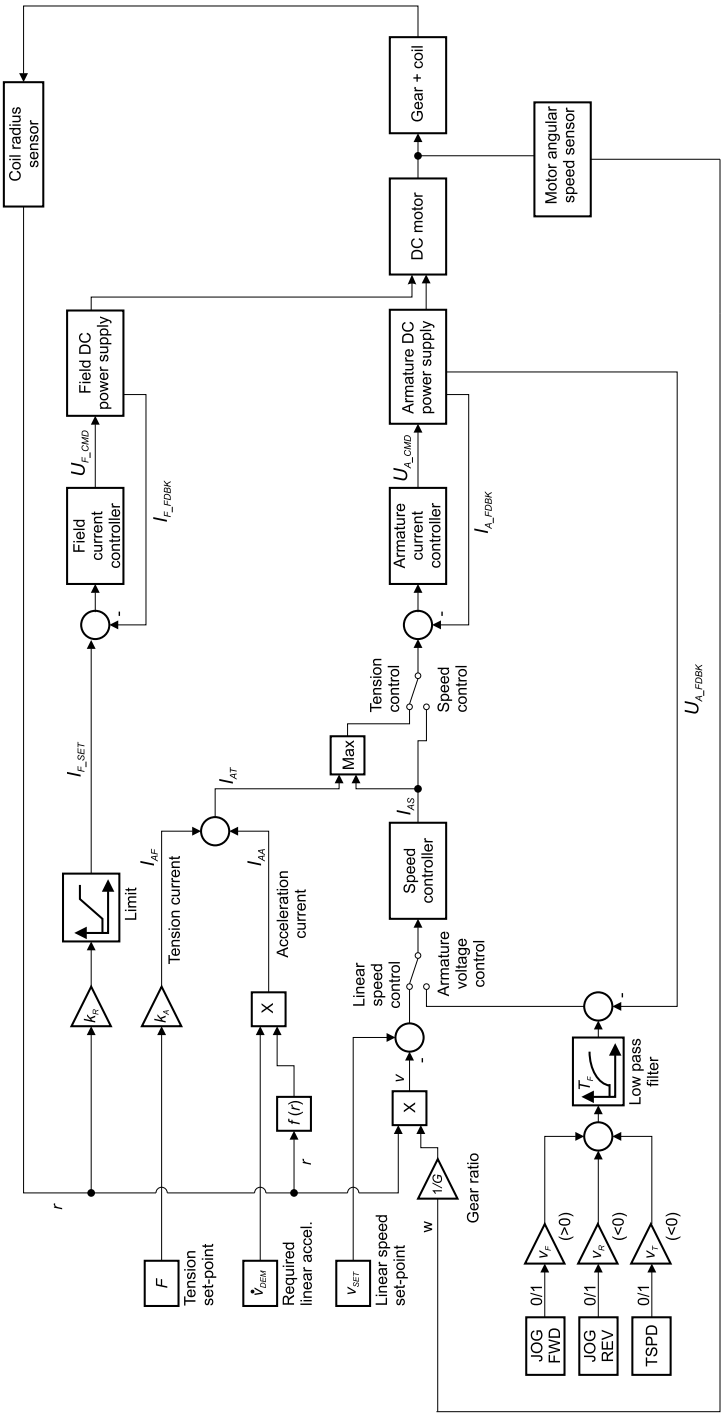

Fig. 7.13 Uncoiler DC drive control block diagram, a simplified view

active. This prevents the speed from increasing in reverse direction in case tension from the slitter is absent or interrupted (e.g., due to a steel strip being torn off). If the tension from the slitter is interrupted, then the armature current tends to approach zero. The armature current controller responds to this and tries to keep the current at the set-point I_{AT} by increasing the armature voltage in a negative direction towards -100 %, which would cause the uncoiler to accelerate in the inverse direction. But once the armature voltage U_{A_FDBK} falls below the safety set-point v_T (-30 %), the armature voltage error becomes positive, which causes the output of the speed controller I_{AS} to increase and become positive too. Consequently, the MAX function selects I_{AS} since it is greater than I_{AT}, which is negative. Since now I_{AS} represents the active armature current set-point, the drive actually switches to speed control mode; the armature voltage and consequently also the linear speed are under control. Without this safety measure, the uncoiler would accelerate in the reverse direction leaving the speed out of control.

Under normal conditions, when there is tension from the slitter the actual armature voltage is negative, but it is greater than v_T (-30 %). Consequently, the speed controller output I_{AS} is at negative saturation (-100 %) since it tends to decrease the armature voltage to v_T. At the same time, the signal I_{AT} is negative too, but greater than -100 %. Since we have ($I_{AT} > I_{AS}$), the MAX function selects the I_{AT}, which means that the armature current controller regulates the tension.

Speed Mode Speed control mode is used in the regime for rewinding the steel strip without slitting. Since this does not fall within the scope of this chapter, it will not be discussed further. Let us only mention that in this case the selection switch in front of the speed controller is set to the position "linear speed control" and the switch in front of the armature current controller is set to the position "speed control". The signal v_{SET} is used as a linear speed set-point, whereas the speed feedback v is calculated from the measured motor angular speed ω by relation (7.21).

Jog Mode Uncoiler jog operation is needed during line start up to feed the steel strip into the line and also during interrupted operation to resolve irregular situations. During jog operation, the operator manipulates the steel strip by rotating the uncoiler forward or backward at slow speed. Movements are controlled via the push-buttons *JOG FWD* and *JOG REV*. The forward and backward jog speed set-points are defined by the constants v_F and v_R. The jog speed set-point is filtered by a low pass filter to obtain a soft start and soft stop. During jog operation, the selection switch in front of the speed controller is set to the position "armature voltage control", which means that the linear speed calculated by Eq. (7.21) is substituted for by the feedback armature voltage U_{A_FDBK}, which is approximately proportional to the linear speed, as follows from relation (7.24). This substitution is needed since at very low speed the operation of the angular speed sensor is not accurate enough, and for short moves its response time may not be adequate.

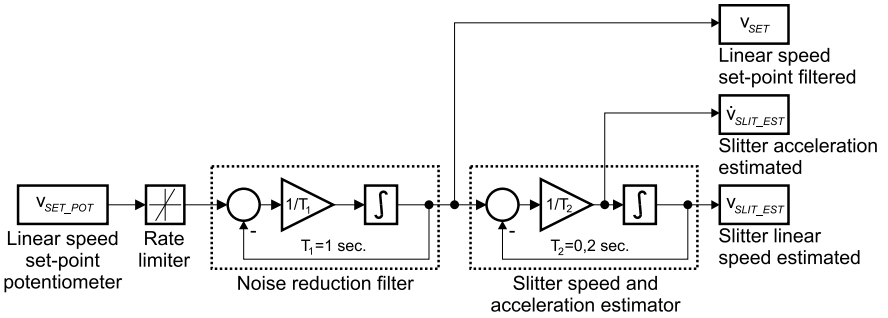

Fig. 7.14 Diagram for processing the speed signal and estimating slitter acceleration

7.4.5 Processing of the Speed Set-Point Signal and Estimation of the Slitter Acceleration

As already explained, the input $\dot{v}_{DEM}$ in Fig. 7.13 represents the required acceleration of the uncoiler and it must match the actual linear acceleration of the slitter as closely as possible. However, the acceleration of the slitter is not measured directly, since the measurement is problematic. In principle, slitter linear speed could be measured by an incremental encoder and linear acceleration could then be calculated by numerical derivation of the speed signal. Unfortunately, this approach poses two problems. Firstly, the derivation amplifies the high frequency noise in the speed signal, and secondly, the calculated acceleration is delayed with respect to the actual acceleration. Both problems would seriously deteriorate the proper operation of the proposed control structure. Therefore, direct measurement of the slitter linear acceleration is substituted for by model-based estimation. The presented block diagram in Fig. 7.14 performs two tasks: first, it processes the linear speed set-point signal, which is adjusted by the operator, and second, it estimates the actual linear speed and acceleration of the slitter.

Let us briefly explain the functionality of the diagram. The input to the diagram is the linear speed set-point signal v_{SET_POT}, which originates from the potentiometer, adjusted by the operator. The signal from the potentiometer is first processed by a rate limiter, which limits the acceleration if the operator readjusts the potentiometer too vigorously. Maximum up and down rates are determined so that the resulting acceleration/deceleration is limited to a value which can be followed by all drives. The next processing step is a noise reduction filter (first-order low-pass filter), which reduces the noise in the speed set-point signal. The output v_{SET} represents the linear speed set-point for all drives, the uncoiler, slitter and recoiler. The noise reduction filter is followed by the slitter speed and acceleration estimator, which represents the simplified model of the slitter dynamics. More specifically, it approximates the dynamic relation between the linear speed set-point v_{SET} of the steel strip and the actual speed of the slitter. It provides the estimated slitter speed v_{SLIT_EST} and the estimated slitter acceleration $\dot{v}_{SLIT\_EST}$, which is then fed into the uncoiler control diagram (Fig. 7.13), i.e., into the $\dot{v}_{DEM}$ input.

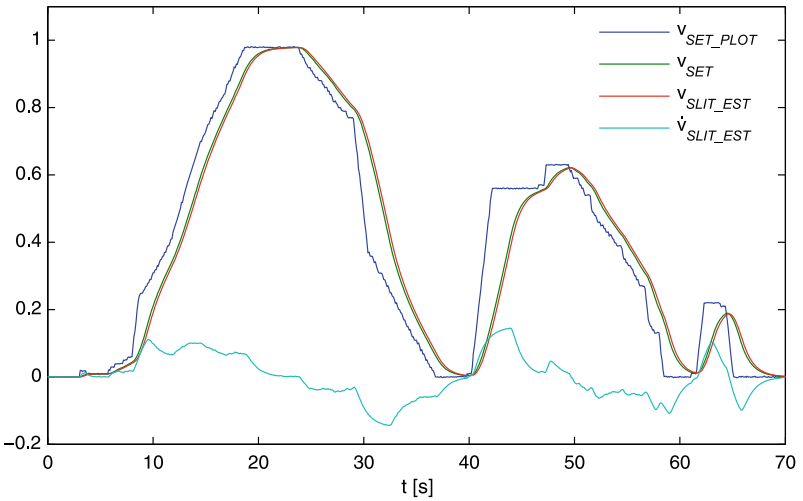

Fig. 7.15 Result of the processing of the speed set-point signal (1 means 160 m/min.)

The estimator is in fact an open loop observer, implemented in terms of a first-order low-pass filter with static gain equal to one. This kind of observer can be used in our case since both static and dynamic observation errors are expected to be small. The static error is expected to be near zero since slitter speed is controlled in a closed loop by a PI controller, which means that the static gain between the linear speed set-point and actual speed equals one. Also the dynamic error is expected to be small, since the acceleration/deceleration is limited by the ramp function and the dynamic delay between the linear speed set-point and actual slitter speed is almost negligible. By trial and error, we found the estimator time constant 0.2 s to be appropriate. The effect of processing is shown in Fig. 7.15.

7.4.6 Estimation of the DC Drive Parameters

Equations (7.33), (7.34), (7.35), and (7.36) represent the feedforward part of the tension control block diagram. They contain several parameters of the DC drive that are unknown. It would be very impractical to determine all parameters by first principles. Therefore, some parameters were estimated from measurements using a grey box modelling approach [8].

To determine the factor k_A between the tension force F and the armature current I_A in relation (7.33), we need to know the motor constants k_0 and k_F, the gear ratio G, and the factor k_R between the field current and the coil radius. The gear ratio G is usually specified on the gearbox data tag, and in our case is

$$G = 18.41 \tag{7.37}$$

The factor k_R between the field current and the coil radius is a control parameter and it was determined in such a way that at the maximum possible coil radius $r = 615$ mm the maximum allowed field current $I_F = 15$ A was applied. The corresponding current field factor in this case is

$$k_R = 24.4 \text{ A/m} \tag{7.38}$$

The next step was to determine the parameters k_0 and k_F. Since in Eq. (7.33) they appear in terms of a product, there is no need to identify each parameter independently. Their product $(k_0 k_F)$ can be estimated by inverting Eq. (7.8) in the following way:

$$k_0 k_F = \frac{U_A - I_A R_A}{I_F \omega} \tag{7.39}$$

The estimation can be carried out by using the armature voltage, the armature current, the angular speed, and the field current, measured while the motor is operating at steady speed without any external load applied. In general, the armature resistance R_A must be also known, since it appears in relation (7.39). However, the expected armature resistance of the considered DC motor is very low (only around 0.1–0.2 Ω) and also the armature current I_A at constant speed and the absence of external load is quite low since it only compensates for the motor and gearbox friction. Consequently, the term $(I_A R_A)$ in Eq. (7.39) can be neglected. At an applied armature voltage of 150 V and field current of 7.3 A, the measured angular speed of the motor was approximately 208 revolutions per minute. From this data we estimated the product $(k_0 k_F)$

$$k_0 k_F \approx \frac{U_A}{I_F \omega} = \frac{150 \text{ V}}{7.3 \text{ A}(\frac{2\pi \cdot 208}{60 \text{ s}})} = 0.94 \text{ Vs/A} \tag{7.40}$$

Once the product $(k_0 k_F)$ is known, it is possible to calculate the factor k_A in relation (7.33), which represents the link between the tension F and the tension current I_{AF}

$$k_A = \frac{1}{k_0 k_F k_R G} = 0.0024 \text{ A/N} \tag{7.41}$$

Since the tension F is not prescribed in terms of a numerical value and the operator adjusts the tension set-point based on experience and visual feedback, determining the factor k_A is not absolutely necessary. However, if k_A is known, an indication of the tension can be provided in engineering units.

Next, it is necessary to evaluate relation (7.34) by determining the function $f(r)$. Using relations (7.35) and (7.36), the function $f(r)$ can be expressed as

$$f(r) = \frac{G}{k_0 k_F k_R} \cdot \frac{J}{r^2} = \frac{G}{k_0 k_F k_R} \left[\frac{\pi l \rho}{2G^2} \left(r^2 - \frac{r_n^4}{r^2} \right) + \frac{J_H}{G^2 r^2} + \frac{J_M}{r^2} \right] \tag{7.42}$$

Note that the moments of inertia J_H and J_M are both unknown. The effective density of the coil material ρ is also not precisely known due to the existence of air gaps between particular turns of the coil.

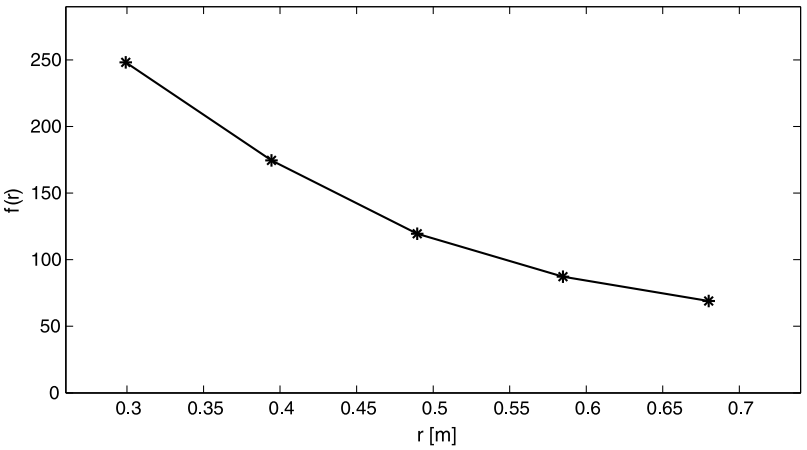

Fig. 7.16 The interpolated function $f(r)$

Based on this, we decided to estimate the function $f(r)$ experimentally and represent it in terms of a look-up table and linear interpolation. The following calibration procedure was used. A steel strip coil was placed on the uncoiler, but the coil remained packed, and a steel strip was not fed into the slitter. The coil radius was measured by the installed ultrasonic sensor and the field current was adjusted accordingly by relation (7.23). Then the set-point of the armature current was changed stepwise from zero to a constant value, which caused the drive to accelerate linearly from zero speed (ramping-up). During acceleration, the linear speed v was calculated following Eq. (7.21) and recorded. We measured the time t_{end} which was needed for the drive to accelerate from zero to the target linear speed v_{end}. Once the target speed v_{end} was reached, the armature voltage set-point was set back to zero and the drive was stopped by a mechanical brake. The value of f was then calculated for a particular radius by dividing the armature current set-point by the calculated linear acceleration ($a = v_{\text{end}}/t_{\text{end}}$)

$$f(r) = I_{A\_SET}\frac{t_{\text{end}}}{v_{\text{end}}} \tag{7.43}$$

In order to build a complete look-up table the procedure was repeated for five different coil radii, starting with the minimum (0.3 m) and ending with the maximum radius (0.68 m). The graph of the function using linear interpolation between particular points is presented in Fig. 7.16.

Due to possible changes and drifts in the process parameters, the function $f(r)$ can gradually become inaccurate and this may lead to poor tension control during acceleration and deceleration. For this purpose, we introduced a multiplication constant c into relation (7.34)

$$I_{AA} = \dot{v}cf(r) \tag{7.44}$$

The constant c can be set by the operator in the range $(0.7 \ldots 1.3)$ via the potentiometer. By this, the operator can correct a possible inaccuracy of the function $f(r)$ until a recalibration is performed.

7.4.7 Tuning the Controllers

Three closed loop controllers can be found on the control diagram in Fig. 7.13: the armature current controller, the speed controller, and the field current controller. All three are implemented as continuous time proportional-integral (PI) controllers. Generally, the control action of the PI controller is determined by two parameters: the proportional gain k_p and the integration time T_i. These two parameters must be tuned to obtain optimal control response. They were tuned experimentally, while the control response was monitored by an analogue paper recorder. The reasons for using such a classical method of controller tuning are explained below in Sect. 7.6.

Tuning the Armature Current Controller The first step consists of recording the response of the armature current to the armature voltage change (square pulses). From this, the orders of magnitude of the PI parameters were determined using standard tuning rules, see, e.g., [2]. After that, the PI parameters were optimised experimentally by trial and error until a fast but oscillation-free response was achieved. Attention was devoted not only to the controlled signal (the armature current I_{A_FDBK}), but also to the control signal (the armature voltage command U_{A_CMD}) and the actual armature voltage U_{A_FDBK}. The time profiles of all three signals needed to be

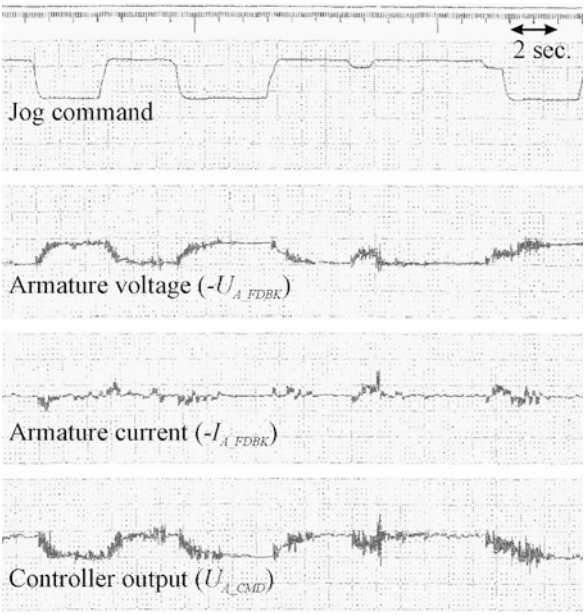

Fig. 7.17 Armature controller operation when the proportional gain was too high

free of oscillations and noise. Experimental optimisation was possible, since the control response was very fast and many parameter combinations could be tested in a very short time. Figure 7.17 shows an example of the operation of the armature current PI controller where the proportional gain was too high. This can be seen from the significant amount of noise in the signals, which can cause problems for the armature DC power supply.

To resolve this problem, the proportional gain was reduced. We found the combination $k_p = 0.5$ and $T_i = 0.2$ seconds very convenient. Note that in Fig. 7.17 the actual armature voltage and current are represented in terms of negative signals ($-1 \cdot U_{A\_FDBK}$ and $-1 \cdot I_{A\_FDBK}$).

The field current controller was tuned in a similar manner, although a lower proportional gain and slower response was acceptable, since the field current set-point changes with the coil radius, which changes relatively slowly.

A similar experimental technique was also used to tune the PI controller for speed; in this case the optimal parameters were $k_p = 2$ and $T_i = 0.5$ seconds.

7.4.8 Testing and Evaluation

During implementation and commissioning, the operation of the system was thoroughly tested. The most important question was if the system would be able to control the tension accurately enough during speed changes (acceleration/deceleration). Since the level of tension is not measured by a sensor, it was not possible to numerically compare the actual tension with the required value. In our case the only possibility was to evaluate the tension visually by monitoring the sag of the steel strip, as shown in Fig. 7.12. The tension was evaluated at both constant and variable linear speed and the visual inspection showed that the system was able to control

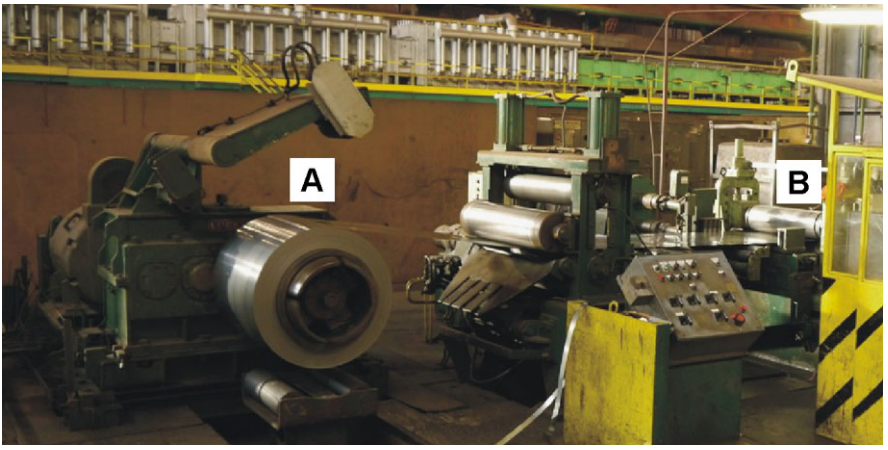

Fig. 7.18 Uncoiler (**A**) and slitter (**B**) during operation

Fig. 7.19 Closer view: a section of the steel strip under tension

the tension within the required tolerance. Figure 7.18 shows the critical section of the steel strip between the uncoiler (A) and the slitter (B) and Fig. 7.19 shows the sub-section of the steel strip in front of the slitter, where the sag of the steel strip can be monitored.

Let us point out that the entire project was successfully completed and the new control system has been in service for several years. The slitting line functionality was expanded for the production of both the thinner and thicker materials and all economic goals were achieved. Thanks to the new control system, the production capacity for the thinner material was increased by almost 100 %. Since the new system was based on the already existing mechanical setup, it represented a relatively modest investment.

7.5 Implementation Issues

For successful implementation of the control system the theoretical analysis and design presented in this chapter had to properly consider many important implementation issues. Some of these will be briefly discussed below.

7.5.1 Selection of the Implementation Platform

The control structure and the corresponding algorithms of the new control system were implemented on a programmable logic controller (PLC). For successful implementation it was necessary to select a PLC with suitable hardware and software capabilities. The following criteria for the selection of hardware and software were the most important:

- *Computational power*. The computational power of the PLC needed to be sufficiently high to guarantee a short enough execution period of the control algorithms. Generally, tasks related to the control of electric variables and also position and motion require fast control responses and thus higher computational

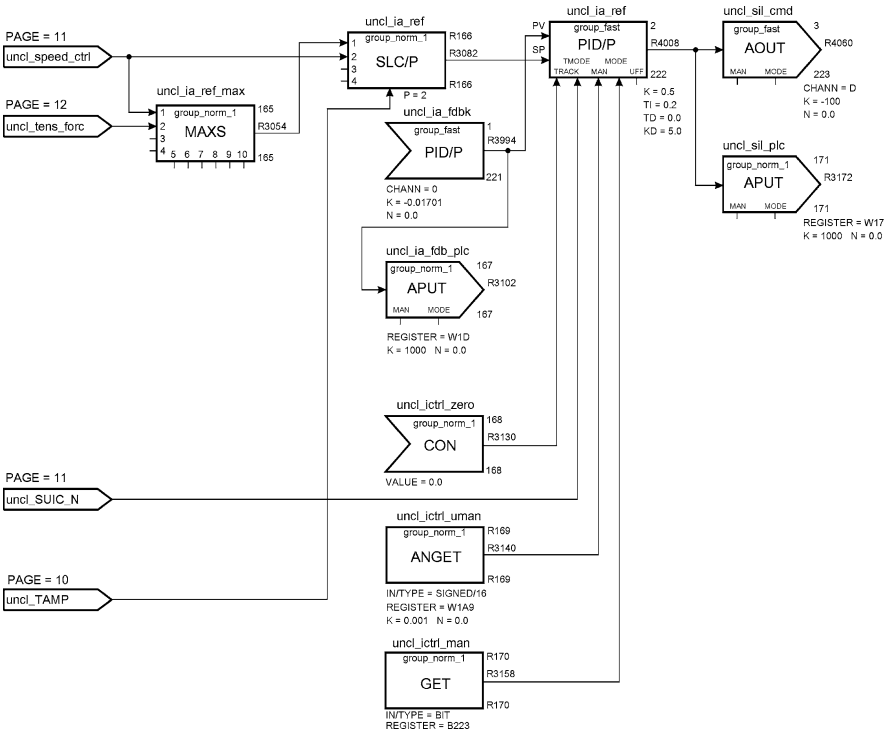

Fig. 7.20 A sample page of the control block diagram

power. All the PI controllers of our control block diagram are implemented as software blocks and the periodic execution of the blocks must be fast enough to mimic continuous operation. Therefore, the selection of an adequate execution period is important. Here we followed the rule of thumb which suggests that the execution period must be at least 5 to 10 times shorter than the time constant of the open loop response of the controlled variable. The most critical is the armature current controller, since the armature current has the fastest response to change in the control signal (the armature voltage). The time constant of the response is determined mainly by the cut-off frequency (30 Hz) of the analogue filter of the armature current signal. This means that the open loop time constant is approximately 33 milliseconds. Therefore, the execution period of the armature current controller was chosen to be 5 milliseconds, which is approximately 7 times shorter than the open loop time constant. By the same rule, we also determined the execution period for other controllers, which was 150 milliseconds.

- *Different execution periods*. Running the complete control block diagram with the shortest execution period (5 milliseconds) would be acceptable, but it would require very high computational power, since the complete diagram is composed of more than 300 programming blocks. To optimise the utilisation of the available

computational power, we introduced two different execution periods for particular parts of the control diagram: a fast one (5 milliseconds) and a normal one (150 milliseconds). As explained above, the fast execution period was only used for closed loop control of the armature currents, while the normal execution period was used for all other tasks, including the control of the mechanical variables (speed, tension, loop level). In general, the option of having several execution periods can be built into the operating system of the programmable logic controller or supported by its programming tool. In our case, a programming tool was used which supported the grouping of the programming blocks into several groups, each group having its own execution period and priority class. Note that there is a strong interaction and dataflow between control functions with fast and normal execution periods. The programming tool must make this communication possible and easy, which may not be the case in classical multitasking structures, where both groups would be implemented in terms of separate programs.

- *Rapid prototyping*. The possibility of rapid implementation and prototyping was very important, since it was expected that during commissioning some parts of the control structure would have to be modified, expanded, or redesigned in a short period of time, possibly without major programming effort, using a graphical interface with the ability to drag and drop the pre-programmed functions from the library. Block-oriented programming tools are preferable for this kind of software development. The designer has the freedom to select the programming blocks from the library, insert them into the control diagram, and connect them with other blocks via input and output signals. Usually, libraries contain pre-programmed blocks and there may also be a possibility to add customised blocks. The benefit of such an approach to software development is the time savings due to the re-use of prepared functions and a significant reduction in programming errors due to the use of checked and approved functions. In our case, we needed the following types of function blocks: arithmetic operations (addition, subtraction, multiplication and division), logic operations, a PID controller, lead/lag, a low pass filter, a look-up table, limitation, rate limitation, a selection switch, a comparator, minimum and maximum selection, and settable numerical constants.
- *Online monitoring and parameter setting*. For effective commissioning, it must be possible to monitor online any selected signal in the control block diagram without any programming effort. At least display in numerical format must be provided and possibly also in terms of a time chart, which is useful to check the responsiveness and stability of control loops. Also online changing of the parameters without the need to compile and download the code is very important.

All the above criteria had to be fulfilled during the selection of the programmable PLC. We selected a modular PLC of Mitsubishi Electric, series A1S with two processing units and a number of digital and analog input/output modules. The first processing unit was a standard unit A1SH CPU used for sequential operations (coordination and switch-over between operating regimes). It was programmed with a

classical ladder logic diagram by using the Mitsubishi Medoc programming tool. The second processing unit was the special coprocessor module SPAC20, designed jointly by Jožef Stefan Institute and the company INEA and marketed by the company Mitsubishi Electric. This unit is fully compatible with Mitsubishi Electric A1S series controllers and is based on a relatively powerful signal processor, the Texas Instruments DSP TMS320C32 with a 40 MHz clock and 2 MB of RAM. It executes the entire control block diagram, organised in the mentioned two groups with normal and fast execution periods. For programming, the block-oriented programming tool IDR BLOK[1] v. 4.22 was used, which satisfied all the above-mentioned criteria and which is produced by the company INEA. Figure 7.20 shows one sample page of the documentation of the program implemented in IDR BLOK, representing the armature current PI controller of the uncoiler. Note that the entire program takes up around 20 pages, containing over 300 programming blocks.

7.5.2 Signal Interfacing

The PLC was connected to the DC power supplies via analogue and digital signals. Custom-designed interface electronics circuits were necessary to connect the standard PLC signals ($-10 \ldots 10$ VDC or $0/4 \ldots 20$ mA) with the non-standard signals of the DC power supplies ($-15 \ldots 15$ VDC or $-25 \ldots 25$ VDC). The PLC and interface electronic circuits were integrated in the signal cabinet, shown in Fig. 7.21. In the first (top) row, the PLC is installed, the second row from the top is occupied by interface electronic circuits, and the remaining bottom rows are occupied by the power supply for the signal lines, fuses and installation material.

7.5.3 Sensors

In general, sensors for the measurement of process variables are important parts of control systems. Special attention must be devoted to their selection and also to their installation. In our case, besides electric variables, the coil radius has to be measured online, since it is needed in the control system to control the field current via relation (7.23) and to evaluate the function $f(r)$. Note that before the upgrade the coil radius had not been measured, so the sensor had to be added for this purpose. The idea was to use a general purpose and relatively low cost ultrasonic distance sensor. However, it turned out that this measurement required special attention. Note that the roundness of the uncoiler and recoiler coils is usually not ideal, but slightly eccentric. This causes the measured distance signal to slightly oscillate while the

[1]The concept of IDR BLOK is closely related to the more recent "Function Block Diagram" of the IEC 61131-3 standard. An IEC 61131-3 compliant version of IDR BLOK has recently been developed.

coil rotates. We tested three different ultrasonic sensors and not all were able to handle the slight oscillations of the distance. Either a frozen or temporarily wrong measurement appeared due to distance oscillation. None of this was tolerable since it would cause significant disturbances in the control of the DC drives. In addition, the oscillations of the radius are directly transferred to the motor field current set-point via relation (7.23), which can cause uneven motor operation. To prevent this, the oscillations had to be eliminated by low-pass filtering. Such filter can be part of the sensor or, alternatively, implemented in the PLC. The time constant of the filter can be relatively long, since during normal operation the coil radius changes relatively slowly. Finally, adequate attention also had to be devoted to the mounting of the sensor, see Fig. 7.22. The sensor must be protected from any kind of physical impact that is likely to occur in a rough industrial environment.

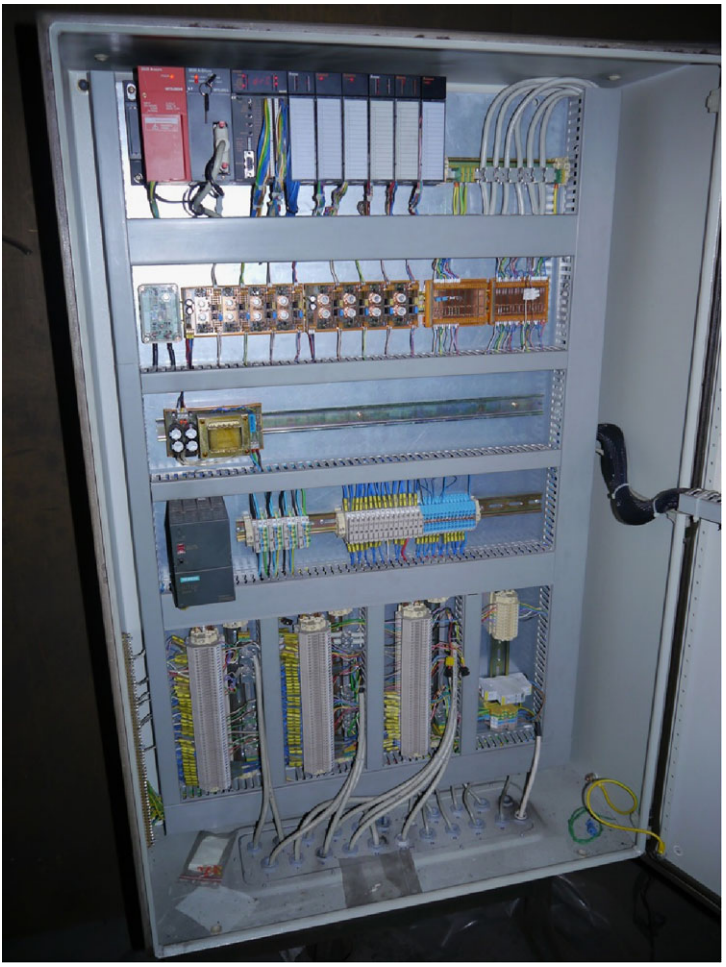

Fig. 7.21 Implementation of the control cabinet

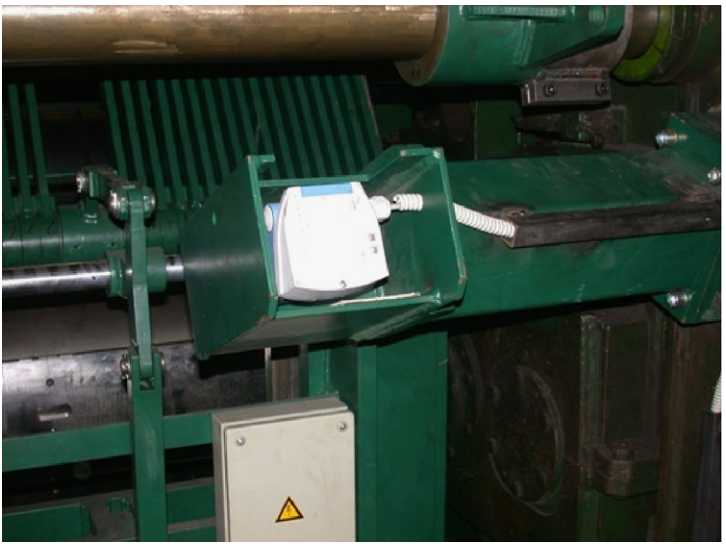

Fig. 7.22 Installation of the ultrasonic sensor for coil radius measurement

7.6 Discussion in the Context of Theory/Practice Issues

The realisation of such a demanding project as the one presented in this chapter is often associated with specific situations which affect the directions in which solutions are sought. Many of them were discussed in previous sections of this chapter. Here we would like to emphasise three additional ones. The first one is related to the analysis of the then existing state (the state before modifications) of the process under consideration, and the other two, to some non-functional requirements which prevented us from applying theoretically more attractive solutions. Let us briefly comment on all of them.

It is well known that the analysis of the then existing state has to be performed at the start of the project [13], and is especially difficult if some existing technical plant is being modified, as in our case. Understanding the existing state represents a foundation for all modifications and improvements. If the existing state is not well understood, the project will most likely fail. In our case, the first and quite rough estimate of the existing state was captured by visual inspection of the slitting line and during valuable communication with the customer's key technical personnel. However, the detailed technical analysis which was needed for the design of the new system and integration with the then existing system could only be obtained from the documentation. This can be a serious problem in general, since the documentation of old systems is often incomplete, inaccurate, with important details missing, and subsequent modifications not documented. In our case, the problem originated also from non-standard documentation nomenclature, which was a consequence of the old age of the slitting line and the fact that the documentation standards at the time of the construction of the line were quite different from today's standards. Con-

sequently, some parts of the documentation were found to be very difficult to understand. Since the documentation did not reveal all the necessary information, many field tests had to be performed to completely analyse the functionality of the then existing system. This was a very time consuming task which substantially affected the design and implementation of the solutions.

One of the basic non-functional requirements of the customer was to provide a low cost system which would be as simple as possible to implement, commission and maintain. Quite often it turns out that advanced methods can be impractical from this point of view. Sometimes, their better performance cannot surmount the difficulties regarding their implementation and exploitation. Let us demonstrate this by two trivial but very evident examples.

In Sect. 7.4.6 we discussed the experimental estimation of the function $f(r)$, which defines the relation between the acceleration component of the armature current I_{AA} and the linear acceleration $\dot{v}$ for different coil radii r. As mentioned, the function was estimated for five different coil radii. At each radius, f was estimated and data points (r_i, f_i), $i = 1 \ldots 5$, were recorded in a look-up table. Based on this table, we wanted to approximate the function f for an arbitrary radius r. Our first thought was to use a polynomial approximation. In this case, the parameters of the polynomial would have to be obtained by a least-squares optimisation method. The main problem was, however, that during commissioning and maintenance it may be necessary to change only a part (possibly only one point at a time) of the approximated function f, leaving other parts unchanged. In the case of polynomial approximation, changing any data point (r_i, f_i) or adding an additional point would require the least-squares optimisation process to be repeated, resulting in a new set of polynomial parameters. Due to the changed polynomial parameters, the complete polynomial is changed. Consequently, also the part of the function f which was intended to be kept unchanged may be changed to some extent, which is very disadvantageous. In addition, we wanted the approximation function to go through all measured points (r_i, f_i), but this cannot be fulfilled in a polynomial approximation and least squares optimisation. Therefore, we decided to use linear interpolation, which does not require any optimisation and allows a change of only a part of the approximated function by simply changing particular data points. In linear interpolation, the approximation function goes through the measured data points, however, in regions between data points it may be somewhat less accurate than polynomial approximation. We found linear interpolation to be much simpler and appropriate for commissioning and maintenance. This rather trivial example illustrates that not only performance, but also implementation, commissioning and maintenance factors need to be taken into account when selecting appropriate methods.

The next example is related to the tuning of the parameters of closed loop PI controllers, which was addressed in Sect. 7.4.7. As explained, we determined the controller parameters manually by repeatedly adjusting them and observing the process response. Based on tuning rules and our experience, we repeated this until the process response was acceptable. Alternatively, we could have used one of the available tools for automatic tuning of controller parameters. These tools determine the controller parameters based on the process dynamic model, which is

automatically estimated from the captured process response to the change of the input signal. Using automatic tuning would by no means be a more exact approach than manual tuning. However, in our case we found automatic tuning less practical. The main reason is that automatic tuning methods usually run on personal computers. It is therefore required that the change of the input signal and process response are recorded by the personal computer. During recording, the sampling period must be sufficiently short to capture the time profile of the process response with enough accuracy. The sampling period should be equal or shorter than the execution period of the controller, which was determined to be 5 milliseconds. Such a short sampling period could hardly be established via the existing serial communication (RS-232) between the programmable logic controller and the personal computer. The lack of communication speed could have been compensated for by buffering the signals in the programmable logic controller and periodic (offline) transmission of the buffer to the personal computer. However, this would have required some additional programming effort, which was not favourable due to the very tight deadlines of the project. Therefore we decided not to use the automatic tuning approach.

7.7 Conclusion

The problem presented in this chapter is tension control in a steel slitting line. It was addressed in the framework of the upgrading of the slitting line. Due to economic reasons and mechanical constraints, established mechanical solutions, such as using a disburdening loop or the application of online measurements of the tension, were not acceptable for the customer. Therefore, alternative solutions were sought.

We proposed an original solution based on feedforward calculation of the armature current of the uncoiler drive, which consists of the tension current and the acceleration current. The tension current is calculated by means of the required tension, which is determined by the operator on the basis of visual inspection of the sag of the steel strip. The acceleration current is calculated from the acceleration of the slitter, estimated by an open loop estimator, and a nonlinear function which incorporates characteristics of the drive and the gear and depends on the changing radius of the uncoiler. The approach has proven to be successful and the designed system has now been in service for several years.

During the design and implementation, the already-known fact that it is very important to fully understand the process before any control system can be designed was confirmed. Understanding the process is as important as understanding the control methodology, however, the background for the control methodology is widely explained in the literature, while the details of the particular process are usually not.

The control system was designed not only for performance, but also for ease of testing, commissioning and maintenance, which turned out to be important not only during start-up and commissioning, but also in later stages of use.

The control system was implemented in the form of software for a programmable logic controller. We composed all control functions from basic control and arith-

metic blocks; no commercially available drive-oriented control software or hardware were used. This method of implementation required a deeper understanding of both the process and the control methodology, but as a benefit, we could provide a solution which was cost effective and fully adapted to the current process.

References

1. ABB Automation Products GmbH. DC or AC Drives? A guide for users of variable-speed drives (VSDs)
2. Åström KJ, Hägglund T (1995) PID controllers: theory, design, and tuning. ISA, International Society for Measurement and Control, Raleigh
3. Carrasco R, Valenzuela MA (2006) Tension control of a two-drum winder using paper tension estimation. IEEE Trans Ind Appl 42:618–628
4. Choi IS, Rossiter JA, Fleming PJ (2007) Looper and tension control in hot rolling mills: a survey. J Process Control 17:509–521
5. Drury W (2001) The control techniques drives and controls handbook. The Institution of Engineering and Technology, London
6. Ebler NA, Arnason R, Michaelis G, D'Sa N (1993) Tension control: Dancer rolls or load cells. IEEE Trans Ind Appl 29:727–739
7. Jeftenić BI, Bebić MZ (2010) Realization of rewinder with a reduced number of sensors. IEEE Trans Ind Electron 57:2797–2806
8. Ljung L (2010) Perspectives on system identification. Annu Rev Control 34:1–12
9. Lynch AF, Bortoff SA, Röbenack K (2004) Nonlinear tension observers for web machines. Automatica 40:1517–1524
10. Sen PC (1990) Electric motor drives and control—past, present, and future. IEEE Trans Ind Electron 37:562–575
11. Shelton JJ (1986) Dynamics of web tension control with velocity or torque control. In: Proceedings of the 1986 American control conference, Seattle, WA, pp 1423–1427
12. Song SH, Sul SK (2000) A new tension controller for continuous strip processing line. IEEE Trans Ind Appl 36:633–639
13. VDI/VDE 3694:2008 (2008) System requirement/specification for planning and design of automation systems. VDI/VDE-Gesellschaft Mess- und Automatisierungstechnik (GMA), Düsseldorf